Materials Science-Poland, 37(1), 2019, pp. 127-135
http://www.materialsscience.pwr.wroc.pl/
DOI: 10.2478/msp-2019-0005

Synthesis and characterization of high-efficiency low-cost solar cell thin film

W. CHRISTOPHER IMMANUEL[1,*], S. PAUL MARY DEBORRAH[2], S.S.R. INBANATHAN[2], D. NITHYAA SREE

[1]Department of Physics, EGS Pillay Engineering College (Autonomous), Nagapattinam, Tamil Nadu, India
[2]Research Department of Physics American College, Madurai, Tamil Nadu, India

Polycrystalline chalcogenide semiconductors play a vital role in solar cell applications due to their outstanding electrical and optical properties. Among the chalcogenide semi-conductors, CdZnS is one kind of such important material for applications in various modern solid state devices such as solar cells, light emitting diode, detector etc. Due to their applications in numerous electro-optic devices, group II-VI semiconductors have been studied extensively. In recent years, major attention has been given to the study of electrical and optical properties of CdZnS thin films. In this work, $Cd_{1-x}Zn_xS$ thin films were prepared by chemical bath deposition technique. Phase purity and surface morphology properties were analyzed using field emission scanning electron microscope (FE-SEM) and X-ray diffraction (XRD) studies. Chemical composition was studied using energy dispersive spectrophotometry (EDS). Optical band gap property was investigated using UV-Spectroscopy. Electrical conductivity studies were performed by two probe method and thermoelectric power setup (TEP) to determine the type of the material. This work reports the effect of Zn on structural, electrical, microstructural and optical properties of these films.

Keywords: *semiconductors; $Cd_{1-x}Zn_xS$; electrodeposition; FESEM; XRD; EDS*

1. Introduction

Sulfides of zinc and cadmium have been used successfully in various optoelectronic devices. The growth of ternary semiconductor thin films have been studied very extensively in the recent years, since these films play an important role in the fabrication of solar cells due to their favorable electrical and optical properties [1]. They are of a great technological interest in heterojunction solar cells and in photoconductive devices due to the fact that cadmium zinc sulfides (CdZnS) thin films have a wide bandgap. The II-VI compounds due to their photoconductivity, found their use in broad applications such as photovoltaic solar energy and thin film transistor electronics [2]. Wide range of polycrystalline semiconducting materials have been studied for the photoconductivity in the visible light. Photodecay and photoresponse properties of photoconductive materials and photovoltaic structures were examined [3]. In this work an attempt has been made to establish the effect of Zn on structural, electrical, micro structural and optical properties of $Cd_{1-x}Zn_xS$ films.

2. Experimental

Physical properties of electrodeposited $Cd_{1-x}Zn_xS$ films are dependent on the deposition parameters such as the bath temperature, relative concentrations of kind of reactants in the solution, pH value and type of substrate. Electrodeposition technique was employed to deposit thin films of $Cd_{1-x}Zn_xS$ on glass substrates. The starting materials, cadmium sulfate and thiourea used were of analytical grade. For the deposition of $Cd_{1-x}Zn_xS$ thin film, a well cleaned glass substrate was immersed vertically in the solution. The temperature of bath was maintained at 70 °C for 3 h. Triethanolamine (TEA) was used as a complexing agent. Ammonia solution was used to maintain the pH of the bath at 10. Finally, the coated substrates were washed with distilled water and annealed at a temperature of 225 °C. The quality of thin

*E-mail: christ.phy@gmail.com

films generally depends on the parameters such as deposition time and temperature of deposition. The deposition parameters employed in this study are collected in the Table 1.

2.1. Structural properties

2.1.1. X-ray diffraction

The phase purity of the film was analyzed with X-ray diffraction (Miniflex, Rigaku, Japan) using CuKα radiation with a wavelength of 1.542 Å.

The structural characterization is very important for explaining structural, microstructural and electrical properties of $Cd_{1-x}Zn_xS$ thin films. The X-ray diffraction patterns were recorded from 20° to 80° as shown in Fig. 1. The XRD analysis revealed that all the films show nanocrystalline nature with cubic phase of $Cd_{1-x}Zn_xS$. The XRD patterns confirm the formation of ternary system alloy $Cd_{1-x}Zn_xS$ with Zn content x = 0.2, 0.4, 0.6 and 0.8, respectively. The compositions were further confirmed using EDS analysis. The presence of sharp peaks indicates crystalline nature of the thin films, from Fig. 1. The observed peaks correspond to the planes (1 0 0), (0 0 2), (1 0 1), (1 0 2), (1 1 0) and (1 1 0) which was found by matching with standard JCPDS data of CdZnS. [7]

The average crystallite size of $Cd_{1-x}Zn_xS$ thin film samples were calculated by using the Scherrer formula:

$$D = \frac{0.9\lambda}{\beta \cos\theta} \tag{1}$$

where, D is average crystallite size, λ is X-ray wavelength (1.542 Å), β is FWHM of the peak, θ is diffraction peak position. The average crystallite size of the samples is presented in Table.

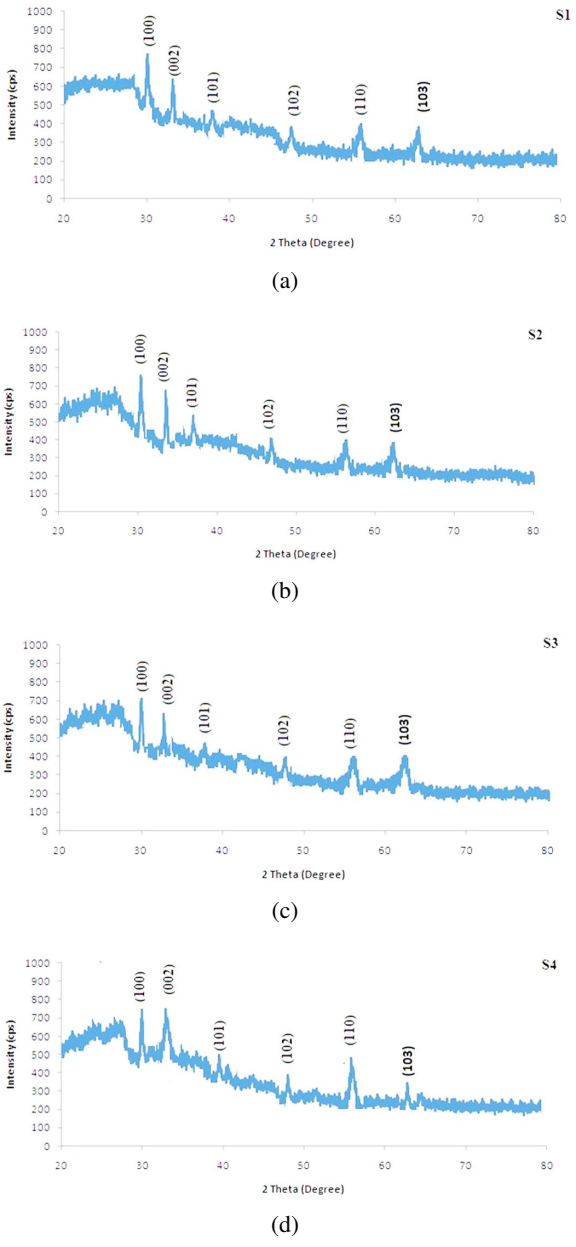

Fig. 1. X-ray diffraction patterns of $Cd_{1-x}Zn_xS$ thin films with (a) 0.2 % Zn, (b) 0.4 % Zn, (c) 0.6 % Zn and (d) 0.8 % Zn.

2.1.2. Field emission scanning electron microscope analysis

The surface morphology of the prepared films was analyzed using a field emission scanning electron microscope coupled with energy dispersive X-ray analysis (EDS) (FE-SEM, JEOL JED 6300).

FE-SEM images of $Cd_{1-x}Zn_xS$ thin films are presented in Fig. 2. The FE-SEM images resolve the nanoparticles associated with the film at high magnification of ×15000. Fig. 2 shows the hierarchical formation [19] of the particle for $Cd_{1-x}Zn_xS$ thin film. Fig. 2d shows agglomerations of the grains. Grain size has been tabulated in Table 3. It is observed that the grain size decreases with an increase in Zn content. The films show a fiber-like morphology as Zn content increases, which may be useful for gas sensing applications.

Table 1. Deposition parameters of $Cd_{1-x}Zn_xS$ thin films.

Deposition parameter	Optimum value/item
Deposition time	70 min
pH	10
Concentration of precursor cadmium sulfate, zinc sulfate, thiourea	0.1 M
Solvent	Deionized water
Zn content [wt.%]	0.2, 0.4, 0.6, 0.8
Deposition temperature	70 °C

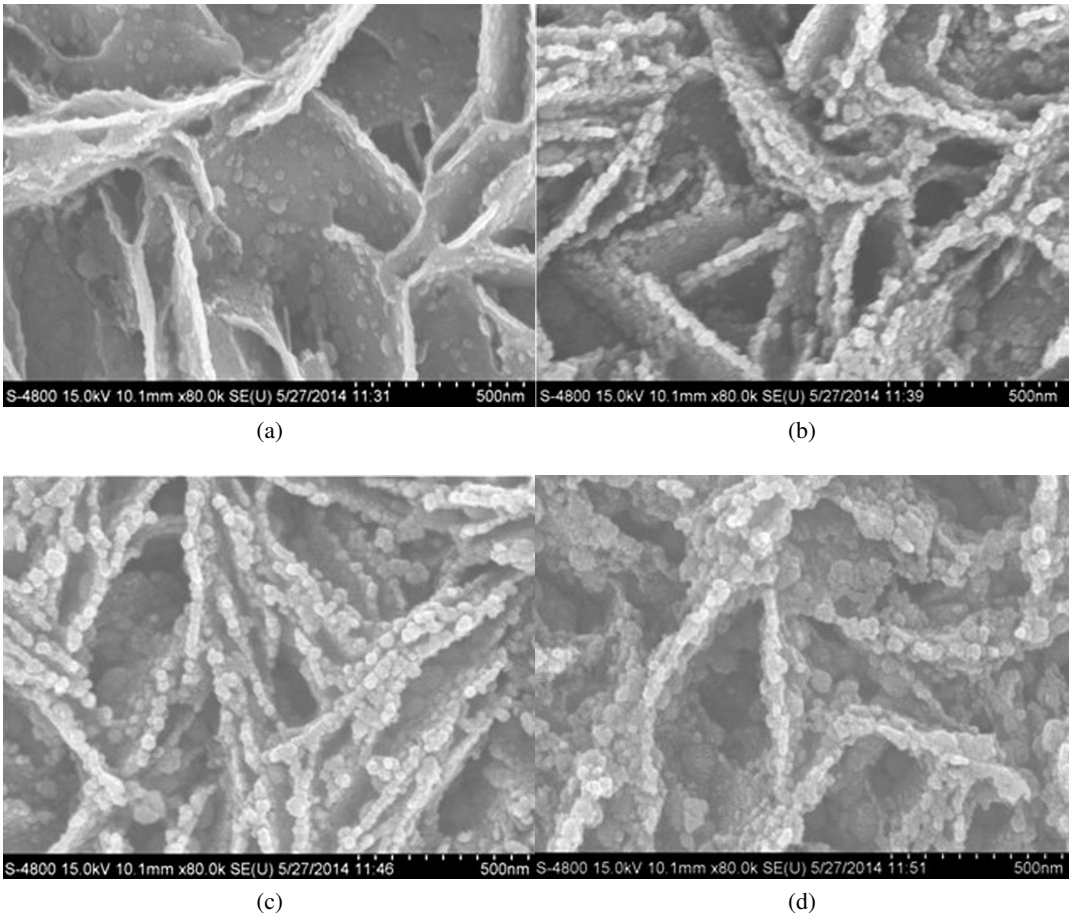

(a) (b)

(c) (d)

Fig. 2. FE-SEM images of $Cd_{1-x}Zn_xS$ thin film for sample S1 (a), S2 (b), S3 (c) and S4 (d)

2.1.3. Quantitative elemental analysis (EDS)

The quantitative elemental composition of $Cd_{1-x}Zn_xS$ thin film was analyzed using an energy dispersive spectrometer. Fig. 3 shows that the prepared $Cd_{1-x}Zn_xS$ thin film is nonstoichiometric in nature.

Table 2 shows that $Cd_{1-x}Zn_xS$ thin films are nonstoichiometric.

2.2. Optical properties study using UV-spectroscopy

Optical absorption studies of hierarchical $Cd_{1-x}Zn_xS$ thin films were carried out in the wave-

Table 2. Quantitative elemental analysis for as-prepared $Cd_{1-x}Zn_xS$ thin films.

Element	Observed							
	S1		S2		S3		S4	
	wt.%	at %	wt.%	at.%	wt.%	at.%	wt.%	at.%
Cd	40.80	33.65	46.65	31.87	48.90	30.68	47.65	29.88
S	18.96	32.80	14.29	32.44	15.21	32.89	13.29	33.61
Zn	40.24	33.55	38.66	35.69	35.89	36.43	39.06	36.51
Total	100.00	100.00	100.00	100.00	100.00	100.00	100.00	100.00

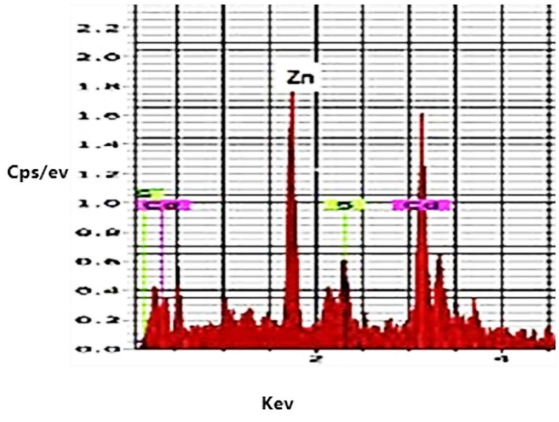

Fig. 3. EDAX of $Cd_{1-x}Zn_xS$ thin film sample (S3).

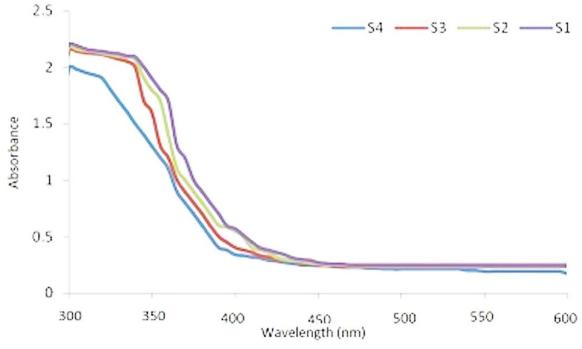

Fig. 4. Variation of absorbance with the wavelength for samples S1, S2, S3 and S4.

length λ range of 300 nm to 600 nm at room temperature, using UV-Vis-2450 spectrophotometer. The change in absorbance with the wavelength λ is shown in Fig. 4. The band gap energies of the samples were calculated from the absorption edges of the spectra [8].

The slope drawn from the start of an absorption edge (the onset of absorbance) and horizontal tangent drawn on absorption minimum intercept each other at some point shown in Fig. 4. The effect of Zn content on the band gap Eg value of the $Cd_{1-x}Zn_xS$ films have been studied. To obtain the band gap value, the absorption coefficient α was calculated from the absorption data. Optical band gap energies of the samples were observed to be slightly varying from 3.55 eV to 3.71 eV [9]. It is well known that a momentous increase in the band gap energy is possible when the size of crystallites reaches the size of the quantum dots. It can be seen that the band gap varies with Zn content in a non-linear way [13].

2.3. Variation of crystallite size, grain size and dislocation density with Zn content

The details of the composition and calculated crystal sizes varying with Zn content are given in Table 3. It is clear from Table 3, that the grain size decreases from 39 nm to 31 nm with an increase in Zn content in the thin films and optical band gap energy increases with an increase in Zn content [4, 8–10]. This may be due to the enhancement in the crystallinity with an increase in Zn content which leads to minimum imperfection. A slight increase in the optical band gap energy of the films with increasing Zn percentage can be attributed to the increase in the crystallite and grain size.

Table 3. Details of % Zn content in $Cd_{1-x}Zn_xS$ thin film, crystallite size, grain size and optical band gap energy.

Sample No.	Zn content	Average crystallite size from XRD [nm]	Average grain size from FE-SEM [nm]	Optical band gap from UV-Vis [eV]
S1	0.2	26	39	3.55
S2	0.4	22	36	3.61
S3	0.6	20	33	3.69
S4	0.8	17	31	3.71

3. Electrical properties

3.1. Thermoelectric power measurements

The p-type or n-type conductivity of $Cd_{1-x}Zn_xS$ thin films was confirmed by measuring the thermoelectric power of the thin film samples. The thermoelectric power TEP was measured as a function of temperature in the range between 320 K and 400 K.

For $Cd_{1-x}Zn_xS$ material, conduction electrons also originate from ionized defects such as oxygen vacancies, rendering n-type conductivity apart from free electrons available. The variation of the thermo emf with temperature difference for all the samples is shown in Fig. 6. TEP increases with an increase in temperature for all samples. $Cd_{1-x}Zn_xS$ thin films were observed to be the n-type material.

3.2. Electrical conductivity

Fig. 7 shows the variation of logσ with 1/T. The conductivity of each sample is observed to increase with an increase in temperature. The rise in conductivity with an increase in temperature implies negative temperature coefficient of resistance and semiconducting nature of $Cd_{1-x}Zn_xS$ thin films. The electrical conductivity of the film decreases with an increase of Zn content. The decrease in electrical conductivity may be attributed to the effect of grain size. The grain size of the film decreases with increasing Zn percentage [11].

3.3. I-V characteristics of thin film of $Cd_{1-x}Zn_xS$ thin films

Fig. 8a depicts the I-V characteristics of Cd_{1-x}ZnxS thin film which is slightly exponential in nature. The I-V characteristics for some samples show that the dark current is negligible, while the current under illumination increases linearly upon increasing the intensity of the light. The contact is ohmic in nature and reveals semiconducting nature of the films.

The variation of photocurrent of $Cd_{1-x}Zn_xS$ thin films with applied voltage is shown in Fig. 8b. The plot shows that there is a linear dependence of photocurrent with applied voltages. The measurement results were analyzed and exposed regions exhibit ohmic conduction mechanism.

Average value of dark resistance is 485 MΩ and it deceases to 100 MΩ, when light is incident on $Cd_{1-x}Zn_xS$ thin film. The $Cd_{1-x}Zn_xS$ films have the highest conductivity for 0.2 % Zn content compared to other compositions.

3.4. Measurement of photoconductivity as a function of wavelength

A plot of photocurrent vs. wavelength of light is shown in Fig. 9. The photocurrent increases with wavelength, reaches a maximum and then decreases. The maximum photoconductivity is observed around 500 nm which corresponds to the band gap of thin films. The photoresponse is observed to decrease both on shorter and longer wavelength side. The decreasing photoresponse on the shorter wavelength side may be due to the surface recombination states. The decrease in photoresponse in long wavelength region is due to cationic vacancies. As the population of these defect levels goes on decreasing above the valence band, the photocurrent decreases with a decrease in energy of the illuminating light [18]. It is seen that for

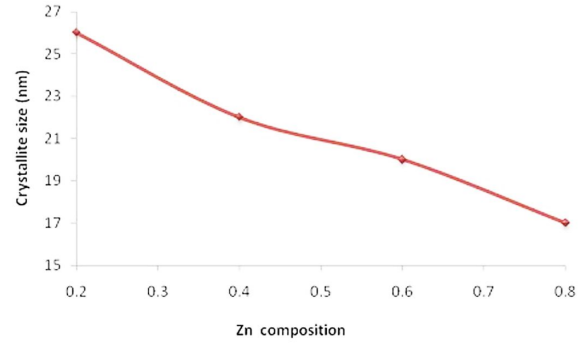

(a)

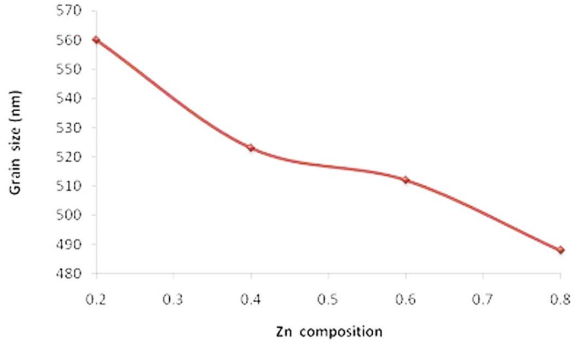

(b)

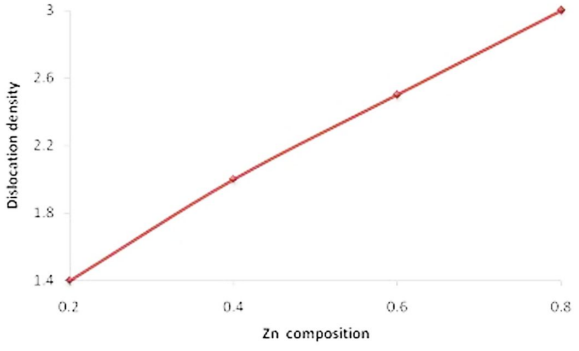

(c)

Fig. 5. (a) Variation of crystallite size with Zn content; (b) variation of grain size with Zn content; (c) variation of dislocation density with Zn content.

lower intensity of light, the slope of the graph is less than unity showing a sublinear behavior which clearly indicates that the photoconductivity of the films is defect controlled. The photosensitivity of $Cd_{1-x}Zn_xS$ is dependent on the wavelength of the incident light.

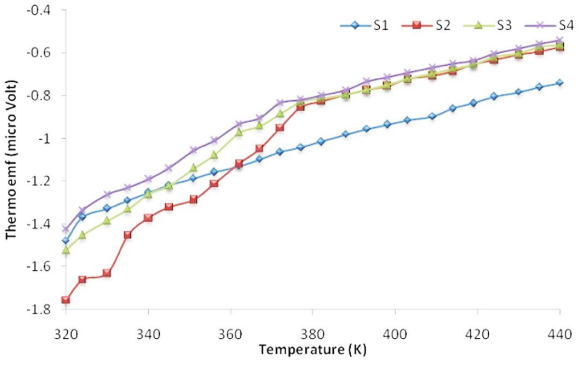

Fig. 6. Variation of the thermo emf with temperature.

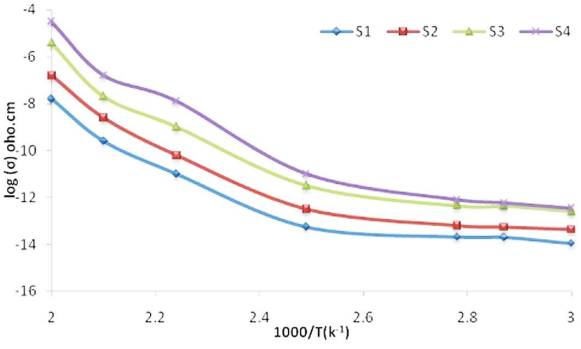

Fig. 7. Temperature dependence of $Cd_{1-x}Zn_xS$ conductivity.

3.5. Measurement of photoconductivity as a function of distance from the light source for different applied voltages

The variation of photocurrent of $Cd_{1-x}Zn_xS$ thin films with varying applied voltage is shown in Fig. 10. The plot shows linear dependence on different distances with different applied voltages.

3.6. Measurement of photoconductivity as a function of distance from light source

From Fig. 11 it is observed that the photocurrent decreases as the intensity of light decreases with increasing distance between the light source and the conductor. It is also observed that the photocurrent is higher in case of blue light than green source of light.

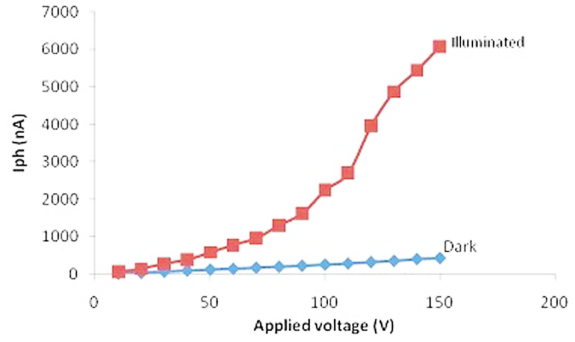

(a)

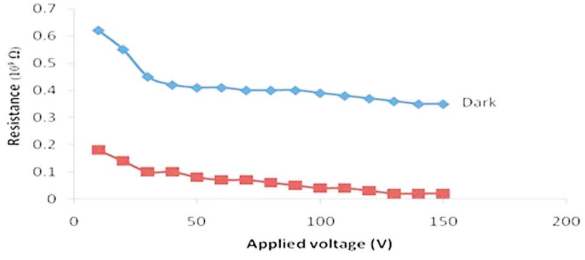

(b)

Fig. 8. (a) I-V characteristics of the films; (b) resistance vs. applied voltage for dark and illuminated films.

3.7. Measurement of resistance as a function of illuminance

Fig. 12a gives a typical example of $Cd_{1-x}Zn_xS$ thin film as a function of incident light. The slope dR/dθ of the curve varies. It is important for detecting anolog-like light level differences. It is seen that for lower intensity of light, the slope is less than unity, showing a sublinear behavior which clearly indicates that the photoconductivity of the films is defect controlled [13–17].

4. Conclusions

The following conclusions are derived from the reported work on effect of Zn percentage on the properties of $Cd_{1-x}Zn_xS$ thin films obtained by electrodeposition technique.

1. The crystallite sizes for $Cd_{1-x}Zn_xS$ films are found to range from 31 nm to 39 nm.

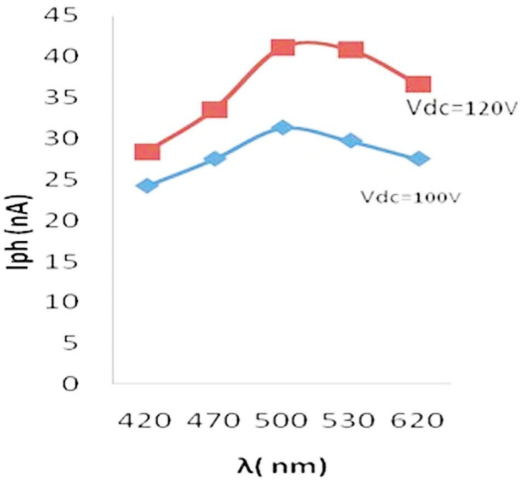

Fig. 9. Photocurrent I_{Ph} vs. wavelength characteristics.

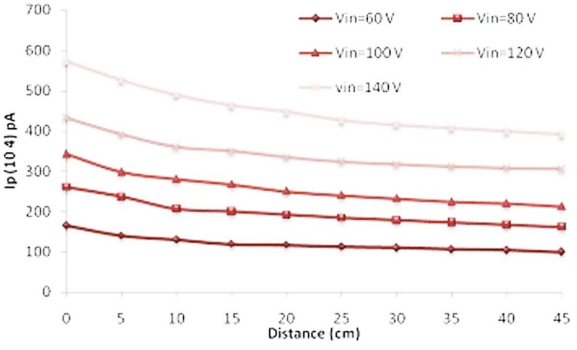

Fig. 10. Variation of photocurrent I_{ph} for $Cd_{1-x}Zn_xS$ thin film with distance from the light source, at different applied voltages.

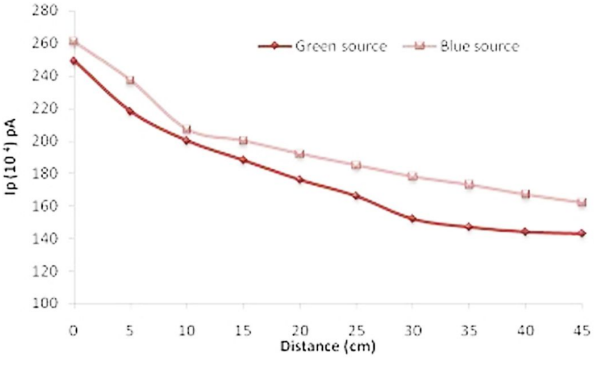

Fig. 11. Photocurrent I_{ph} of $Cd_{1-x}Zn_xS$ thin film vs. distance from different sources of light

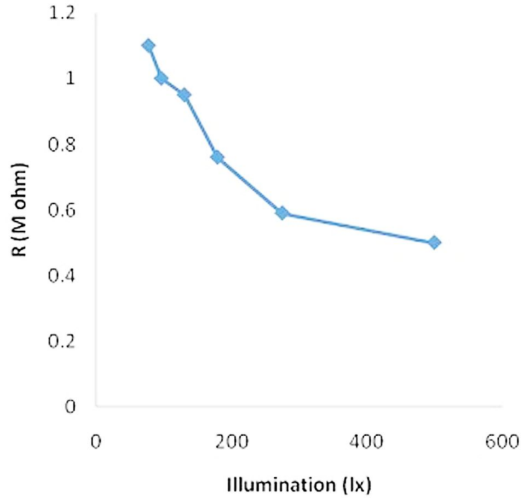

(a)

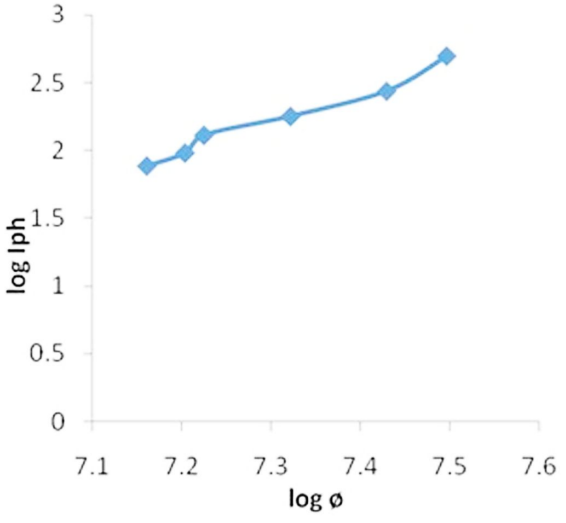

(b)

Fig. 12. (a) Resistance vs. illuminance curve; (b) photocurrent I_{ph} vs. light intensity θ characteristics.

2. The chosen deposition parameters produced $Cd_{1-x}Zn_xS$ thin films of good homogeneity, with varying Zn percentage.
3. The peak analysis from the XRD patterns showed formation of $Cd_{1-x}Zn_xS$ thin films, confirmed by EDS data.
4. The study suggests that the increase in Zn percentage in the film leads to an increase in crystallite size, grain size and optical band gap.
5. Morphological studies of the films confirmed that the as-prepared $Cd_{1-x}Zn_xS$ thin films are composed of hierarchical rod-like structure. The films also reveal fiber-like structure as Zn content increased, which may be useful for gas sensing applications.
6. The elemental analysis confirmed that the as-prepared $Cd_{1-x}Zn_xS$ thin films are non-stoichiometric in nature.
7. Electrical conductivity increased with an increase in temperature of the $Cd_{1-x}Zn_xS$ thin films, indicating their semiconducting nature.
8. TEP measurement indicated that the as-prepared $Cd_{1-x}Zn_xS$ thin films are of *n* type.
9. All samples exhibit photoconductive effect when excited by a light source. The $Cd_{1-x}Zn_xS$ photoconductor behaves like an ohmic resistance that depends upon the intensity of source light. These results will have a significant impact on the use of $Cd_{1-x}Zn_xS$ semiconductors in optoelectronics devices.

References

[1] TYAN Y.S., *Sol. Cell.,* 23 (1988), 59.
[2] SHASHIBHUSHA N., CHANDR T.A., *Turk. J. Phys.,* 32 (2008), 21.
[3] PISARKIEWICZ T., *Opto-Electron. Rev.,* 12 (2004), 33.
[4] CELALATTINBAYBUL M., NILGUNORTHA N., *Thin Solid Films,* 518 (2010) 1925.
[5] NAGAMANI K., REDDY M.V., LINGAPPA Y., RAMAKRISHNA K.T., REDDY R., MILES W., *Int. J. Opto-Electron. Eng.,* 2(2012), 1.
[6] CLEMMINCK I., BURGELMAN M., CASTELEYN M., DEPUYDT B., *Int. J. Solar Energ.,* 12 (1992), 67.
[7] SINGH S., SHRIVASTAVA A.K., *Int. J. Innov. Res. Sci. Eng. T.,* 3 (2014), 1.
[8] SANAP V.B., PAWAR B.H., *J. Opto-Electron. Biomed. Mat.,* 2 (2011), 39.
[9] SHARMA T.P., PATIDAR D., SAXENA M.S., SHARMA K., *Indian J. Pure Appl. Phys.,* 44 (2006), 125.
[10] SELMA M.H., JAWAD A., *Eng. Tech. J.,* 31 (2013), 1.
[11] MAHDI M.A., *J. Basrah Res.,* 35 (2009), 1.
[12] LI W., YANG J., SUN Z., FENG L.-H., ZHANG J.-Q., WU L., *Int. J. Photoenerg.,* 214 (2011), 5.
[13] KAWAR S.S., HURDE K.K., PACHKAWADE A.P., PAWAR B.H., *Int. J. Basic Appl. Res.*, 5 (2012), 157.

[14] SHARMA T.P., PATIDAR D., SAXENA M.S., SHARMA K., *Indian J. Pure Appl. Phys.,* 44 (2006), 125.
[15] BORASE S.V., CHAVAN S.D., SHARMA R., *J. Alloy. Compd.,* 436 (2007), 501.
[16] RAVANGAVE L.S., BIRADAR U.V., MISAL S.D., *Glob. Res. Anal.,* 2 (2013), 1.
[17] MOSIORI C.O., NJOROGE W., NANDOKUMU J., *Dir. Res. J. Chem. Mat. Sci.*, 2 (2014), 13.
[18] PATIL R.H., PATIL S.N., NIKAM S.V., LADGAONKAR B.P., *Int. J. Adv. Eng. Technol.,* 6 (2013), 688.
[19] UBALE A.U., CHIPADE K.S., BHUTE M.V., RAUT P.P., MALPE G.P., SAKHARE Y.S., BELKHEDKAR M.R., *Int. J. Mater. Chem.,* 2 (2012), 165.
[20] SANDHYAPILLA I., BHUSHANB S., *Proc. Nano Thailand*, 2012.

Received 2018-07-19
Accepted 2019-01-09